Journal of Traffic and Transportation Engineering 3 (2015) 178-185
doi: 10.17265/2328-2142/2015.03.006

Buckling Characteristics of Cylindrical Pipes

Toshiaki Sakurai

College of Science and Engineering, Iwaki Meisei University, Fukushima 970-8551, Japan

Abstract: This paper describes the buckling pattern of the body frame by energy absorbed efficiency of crashworthiness related to research of the buckling characteristics of aluminum cylindrical pipes with various diameters formed mechanical tools. Experiments were performed by the quasi-static test without lubrication between specimen and equipment. According to the change in the radius versus thickness of the specimen, the buckling phenomena are transformed from folding to bellows and the rate of energy absorption is understood. In crashworthiness, frames are characterized by the folding among three patterns from the absorbed energy efficiency point of view and weight reduction. With the development of new types of transport such as electric vehicles, innovated body structure should be designed.

Key words: Passive safety, crashworthiness, body structure, body frames.

1. Introduction

This is to explain the result of quasi-static compression buckling test with unlubricated condition by using cylindrical pipes with standardized outer diameter and variable inner diameter with mechanical processing. With a traditional cylindrical pipe buckling observational study, three types of patterns in bifurcation buckling pipe category have been presented. Also, under consideration of front or rear frame energy absorption in automobile body structure for crashworthiness, due to the thickness being relatively thin, the buckling mode, either folding type or diamond type, was found. Additionally, here, cylindrical pipes are being used. However, we understand that, as a result, a hollow pipe with infinite number of edge lines becomes a cylindrical pipe. Historically, an automobile body structure started out with a carriage structure as framing structure became semi-monocoque structure up to the present. With recent appearance of EV (electric vehicle) made downsizing of automobile body structure, tailored blanking is applicable to today's body structure, and new innovation in productive technology such as dissimilar metal welding and bonding, body structure must change as well.

Therefore, with this research, the transition range of deformation mode was figured out by sorting out the past cylindrical pipe buckling mode with radius (r) and thickness (t). By this fact, the case of crash impact energy absorption factor increase will be permitted.

2. Background

Under the historical point of view, the body structure of passenger vehicle started out from horse-drawn carriage style into frame construction, then to semi-monocoque structure by utilizing part of exterior body panel and spot welding like a hat shape frame to the area. As today, it is an energy-absorbing structure in reference to crashworthiness, references listed only in the main paper. Compared to the primary pure monocoque shell, the semi-monocoque shell is applied with reinforcement or stiffener materials. For example, compared to semi-monocoque shell as airframe, automobile body has quite a few open cross-sections. However, it is in a category of semi-monocoque shell. Recently, with improvement of designing and production technology, such as downsizing with launching of EV or new style structure, tailor welded blanking and dissimilar metal welding and bonding, and so forth. We believe that

Correpsonding author: Toshiaki Sakurai, Dr., professor, research field: mechanical engineering. E-mail: sakurait@iwakimu.ac.jp.

now is the time to have a reconsideration about automobile body structure. From the crashworthiness stand point, the body structure has been designed and developed by implementing acceleration characteristics to protect passengers as well as restraint unit with operation timing and vehicle crushable length and energy absorption. From the frame buckling point of view, by weight reduction and streamlined structure, the frame buckling mode is non-axisymmetric deformation which is a folding mode. According to the research result of each OEM's (original equipment manufacturing's) crash data by the Society of Automobile Engineers of Japan, it seemed as it should have become a folding mode from the beginning [1].

However, a folding mode is unstable buckling involving its wall surface buckling and the energy absorption ratio is worse than axisymmetric mode. As buckling phenomenon, there are bifurcation buckling, snap-through buckling and branching buckling. In the group of bifurcation buckling, there is a basic theory that is continued as being considered a column as automobile frame.

Long time ago, the column buckling research was studied by Euler [2]. As today, a column buckling is calculated as with the formula by Euler in 1757 [2, 3] as shown below:

$$C\frac{\mathrm{d}^2 y}{\mathrm{d}x^2} = -Py \tag{1}$$

where, C is an absolute elasticity and P is the buckling load.

From the formula above, another formula to figure out a limit load was easily induced. The buckling study researched by Euler was advanced to buckling study of plate and circular cylinder, and followed by tangent modulus theory by Engesser [2] in 1889, as well as equivalence coefficient theory by Shanley [2] 60 years later in 1947. However, it settled with Engesser's tangent modulus theory [4]. Under the theory, it is to develop buckling deformation starting point and the deformation after buckling can be figured out with non-liner equation as a finite deformation. Also, as we talked about, the bifurcation buckling mode of cylindrical pipe is known for axial symmetry and non-axisymmetric buckling [4, 5].

As a cylindrical pipe buckling equation, assuming Euler buckling does not occur, we use the Donnell equation [5] below:

$$\begin{aligned} &D\nabla^8 w + \frac{Et}{r^2}\frac{\partial^4 w}{\partial x^4} \\ &= \nabla^4\left(N_{x0}\frac{\partial^2 w}{\partial x^2} + 2N_{xy0}\frac{\partial^2 w}{\partial x \partial y} + N_{y0}\frac{\partial^2 w}{\partial y^2} + p\right) \end{aligned} \tag{2}$$

where, $D = Eh^3/12(1 - v^2)$; E: Young modulus; v: Poison's ratio; h: height; $\nabla^2 = \frac{\partial^2}{\partial x^2} + \frac{\partial^2}{\partial y^2}$; w: displacement; N_{x0}: axial force; N_{y0}: circumference power; N_{xy0}: shear force; p: internal pressure.

In the case of axial symmetry, Eq. (2) is linear equation with respect to w when internal pressure p = 0 as condition, and buckling load as eigenvalue problem can be solved. Eq. (3) is satisfied with $w = 0$ and $M_x = 0$ given at the simply supported boundary condition $x = 0$ and $x = l$.

$$w = c\sin(m\pi x / l) \tag{3}$$

Substitute Eq. (3) for Eq. (2), then the critical stress σ_{cr} is obtained. Furthermore, if operating minimum method is related to wave number, Eq. (4) is obtained:

$$\mathrm{d}\sigma_{cr} / \mathrm{d}(l / m) = 0 \tag{4}$$

Then the minimum buckling load is given with the following equation:

$$\sigma_{cr,\min} = \frac{E}{\sqrt{3(1-\nu^2)}}\frac{t}{r} \tag{5}$$

where, $\sigma_{cr,\min}$: minimum critical buckling load; t: thickness; r: outer-radius of cylindrical pipe.

For reference, the following is a plate buckling equation:

$$\sigma_{cr} = \sigma_e k\,,\quad \sigma_e = \frac{\pi^2 E}{12(1-\nu^2)}\left(\frac{t}{b}\right)^2 \tag{6}$$

Eq. (6) (right side forward section) is composed with modulus of longitudinal elasticity E as material constant and Poisson's ratio v, and backward is thickness and curvature radius. That means that a

buckling limit is determined once the material is decided, buckling limit load gets composed with geometric forms. Same with plate buckling, buckling limit load is composed with geometric configuration shown in Eq. (6).

This study shows that by arranging radius and thickness of past cylindrical pipe buckling mode, threshold value of deformation mode and transition value were figured out. By this fact, it is acknowledged that, in case of the efficiency of crash, the energy-absorbing is increased. There are bifurcation buckling, snap buckling, and branching buckling and in the bifurcation buckling. On the other hand, there are three types of buckling such as bellows type, folding type and diamond shape type based on the column theory.

3. Test Method

3.1 Items for Testing

Using commercially available aluminum alloy 5,000 (Al-Mg type), we created the specimen by precise cutting work. The mechanical characteristic of specimen was not required since no tension test was conducted, however, by a metal handbook, longitudinal elastic modulus is 70 GPa and tensile strength is approximately 200 MPa.

Three types of outer diameter ϕ40, ϕ50 and ϕ60 were prepared, and r/t was changed as needed by machine processing.

Fig. 1 shows the drawing that indicates direction. By ϕA and ϕB, the plate thickness can be varied, so material needs to be fabricated. Geometrical tolerance and size tolerance such as alignment, flatness, parallelism, and square are instructed. Also, chamfered edge face should be cut by using the throw-away chip with 0.1 mm denoted ^{C}0.1 in Fig.1. Three diameters per type were prepared and total of 81 cylindrical pipes were created. Outer diameter, inner diameter and the ratio of radius and thickness (r/t), and fabrication instruction size of typical specimen are indicated in Table 1. As indicated in Fig. 1, the accuracy of finishing of thickness size tolerance is ±0.05. So, be aware after selecting various r/t, as a result, if in case values are close, there is a possibility that maximum and minimum tolerances would be a little bit overlapped.

3.2 Test Equipment

The universal tester that is used for quasi-static compression test is from the corporation and was used as displacement control method. The main specific requirement is that testing speed is 0.1~76 mm/min, atmosphere temperature is about 10~38 °C. At this time, with the quasi-static compression test, the compression speed is 3 mm/min, the temperature is approximately ±15 °C and they satisfy the requirement.

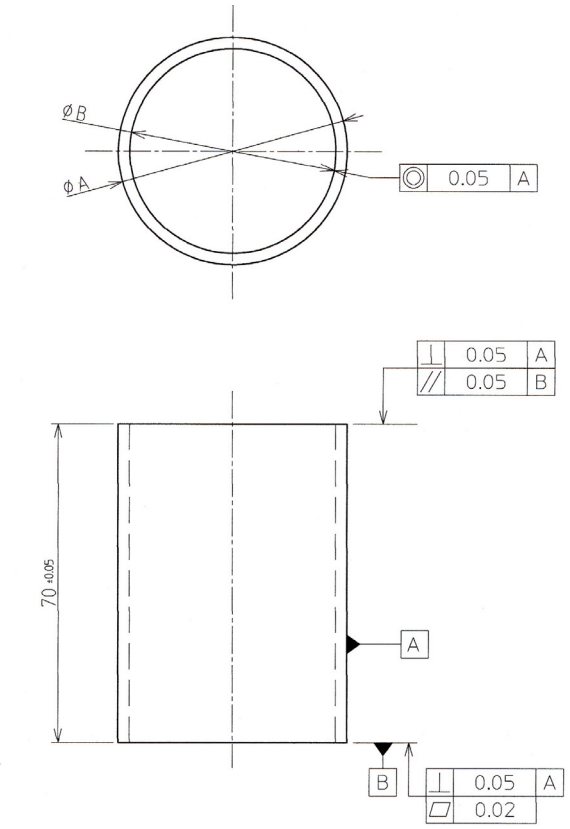

Fig. 1 Drawing for mechanical forming (units in mm).

Table 1 Typical diameter, thickness, ratio of r/t of specimen.

Outer diameter (ϕ)	60	60	60
Inner diameter (ϕ)	54	57.5	57.7
Thickness (mm)	3	1.25	1.15
Ratio of outer radius and thickness (r/t)	10	24	26

3.3 Boundary Condition

When installing test items to the test equipment, the boundary condition regarding frictional condition becomes important. Quite frequently used test items for static buckling test were connected to end plates with certain thickness plate on end with weld construction method. It can be more beneficial if we just select test items with only the accuracy by considering end plate parallelism and deformation after welding. Here, as tentative experiment, we have been considering boundary condition with or without lubricant. Main items for test equipment side with crosshead or bed is that a compression test is being conducted with: (1) wiped with acetone or cleaner solution; (2) lubrication (SAE 10W, ISO32); and (3) Teflon sheet with its thickness 0.5 mm. With the first one, the diameter of test specimen before and after the test was the same. However, testing when lubrication was used, with large plate thickness, it deformed in a concentric fashion, but with thin plate, torsional load was added to the testing plate, and strain and deformation occurred. We also confirmed that under the early stage loading, pure axial force was not loaded. Therefore, future test should be conducted with boundary condition of non-lubricated surface condition of crosshead and bed by wiping with acetone solution. However, at the beginning of the testing, the lubricant and Teflon sheet are properly working as boundary lubrication, but the lubricant condition is uncertain as the test progresses. Observation after the testing showed some damage on the Teflon sheet along the outer diameter of cylindrical pipes.

4. Test Result

4.1 Primitive Transformation—Capacity Chart

Fig. 2 indicates a typical displacement—loading curve. Horizontal line shows displacement (mm), and vertical line shows force (kgf) by the software of test equipment. Outer diameter of the pipe is 40 mm, therefore, the ratio r/t is 24 with plate thickness being 0.85 mm.

Fig. 3 indicates some photos of typical deformation status of Fig. 2. Here, the outer diameter is 40 mm, the ratio of r/t = 24, the thickness is 0.85 mm. Compression status and deformation status as shown in Fig. 3 are qualitatively indicated:

(1) Transition from elastic to plastic range: When transition begins from elastic range to plastic range, it rises up as line shape, reaches elastic limit, and after that, it reaches to the maximum load, moderately elevated. This area is the transition range from elastic

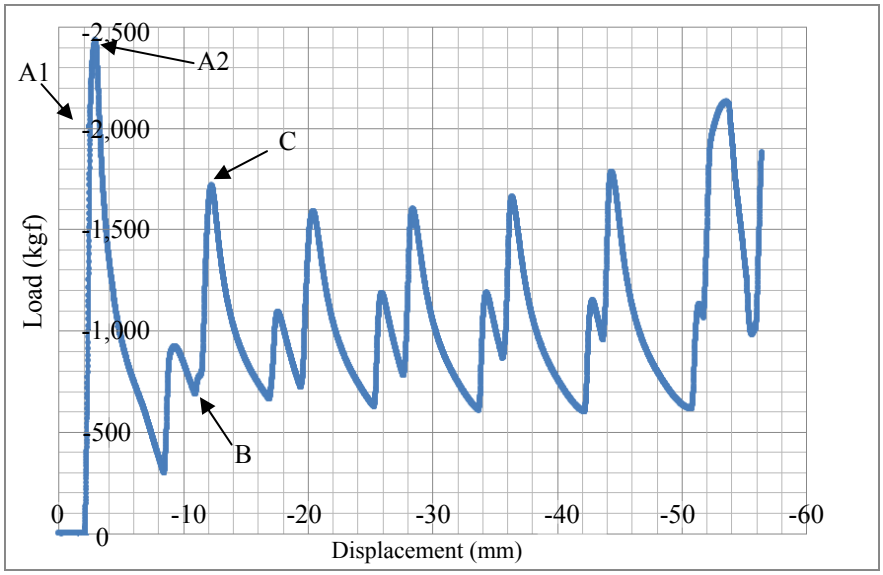

Fig. 2 Typical displacement-load curve in compression load.

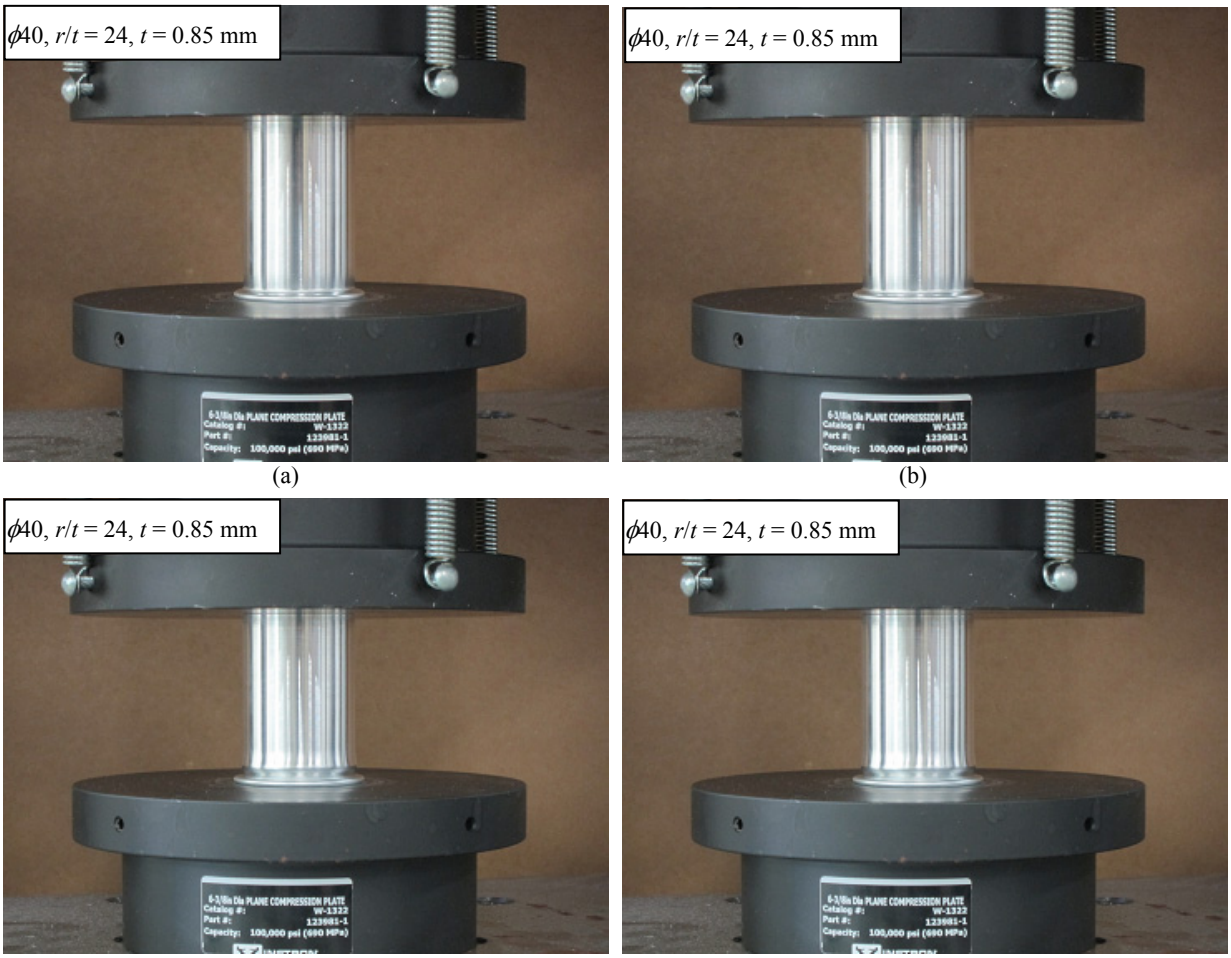

Fig. 3 Typical configuration of buckling: (a) transition from elastic to plastic area (A1); (b) maximum load formed after elastic area (A2); (c) forming of valley (B); (d) forming of mountain peak (C).

to plastic range. Initial bellows shape puffs up towards outside and deforms. Incidentally, first deformation occurs by the bed side. Thus, two photos shown in Fig. 3 are indicated on A1 and A2;

(2) Forming of valley: Maximum load comes up to certain level, then, it comes down as load gets decreased and increased again. This is how to deform valley like to bellows shape forms inside;

(3) Forming of mountain peak: After the valley is formed, loading is increased again, and when it becomes larger than the loading at valley forming, it continues to decrease again. This is how mountain peak is formed.

We found the following factors per area from transformation-capacity chart and these pictures (Fig. 3):

(1) Deformation process to maximum loading which means the process from elastic to plastic range, first the displacement is 0.4 mm, up to loading 20.6 kN (2,100 kgf), it is straight line shape. At this time, the rate of spring is k = 51.5 kN/mm, stress is 200 MPa. After that, the gradient to displacement becomes gentle, and at 23.8 kN (2,430 kgf), it becomes maximum loading. At this point, the rate of spring is k = 8 kN/mm, stress force is 228 MPa. After that, the loading rapidly drops and decreases up to the maximum loading of 3 kN (13%). Deformation occurs as first bellow shape of the first mountain is created. Beginning point is either crosshead side (top of the test piece) or bed side (bottom of the test piece). With this test, it was created from the bed side. The radius of created bellow top was approximately ϕ44.5;

(2) The creation of valley occurs when maximum loading is created and after rapid decrease of loading occurs, then, right when loading goes up again. By observation during the test and from photos, we can confirm the condition of transforming from central axis of the cylindrical pipes plate thickness to internal side. Load increases as valley is being created. When the valley top gets created, the loading goes down. The maximum load at valley creation is 9 kN and inner diameter of bellow ϕ36.5;

(3) After the first valley is created, load gets decreased once, but the volume of the decrease is not large and the load increases again. After the second mountain is created outside, the load then decreases.

At that time, the maximum load is 17 kN and the outer diameter of the mountain top was ϕ44.5 which was the same as previous mountain diameter. The range of A1 and A2 is a phenomenon that occurs only after the initial buckling, however B and C afterword are repeated phenomena. Also, from a mountain to another one, the length of one pitch in this case is 8 mm. However, it means one large mountain created by maximum loading and small valley formations and small mountains followed by that. The number of valley and mountain relates to *r*/*t*. So far, there have not been any research reports regarding valley formation indicated.

4.2 Results Compiled by r/t

By previous Authors' researches [5, 6], buckling mode of cylindrical pipes compiled by *r*/*t* ratio was predictable. The target of this time is to figure out transitional range of deformation mode, another word, and threshold value from bellow deformation to folding mode or mixed material mode including bellow type and folding.

Fig. 4 indicates each displacement loading curve as a whole when using ϕ60 for outer diameter and changing internal diameter by 10 types. This is a representative example for testing with one kind and three test materials. There was not much difference among the three tested materials. When board thickness is reduced, in this case, at *r*/*t* = 24~26, the repeated relationship of deformation and loading is discontinued. At *r*/*t* = 24, all bellow modes are deformed, and at *r*/*t* = 26, mixture of partly bellow and folding mode is deformed which means part of bellow mode was transitioning to folding mode. Additionally, by reducing thickness of the board, the condition becomes evident.

As we can see in Fig. 4, there are nine types of results with different number of mountains.

Table 2 indicates the main ratio of *r*/*t* and number of mountains.

Fig. 5 indicates two patterns: One is complete bellows mode shown in Fig. 5a and the other is mixed mode with bellows mode and folding mode shown in Fig. 5b. At ϕ60, considering 1 for maximum loading of bellows mode with *r*/*t* = 30, corresponding average loading 0.4 for bellows mode, when folding mode occurs at *r*/*t* = 26, average loading becomes around 0.25. As previously said, we can understand that energy absorbing efficiency is not so high.

Table 3 shows threshold of transitional range from bellows mode to mixed modes with bellows and folding patterns due to *r*/*t*.

As shown in Table 3, the ratio *r*/*t* of the transitional range is close to 24.

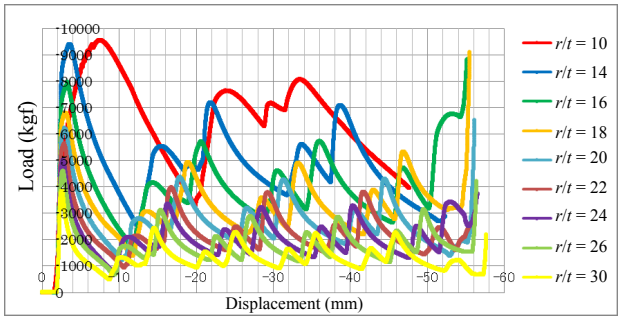

Fig. 4 Summarized displacement vs. load curves.

Table 2 Comparison between the ratio of *r*/*t* and number of mountain.

The ratio of *r*/*t*	10	16	20	24
Number of mountain	3	4	4	5

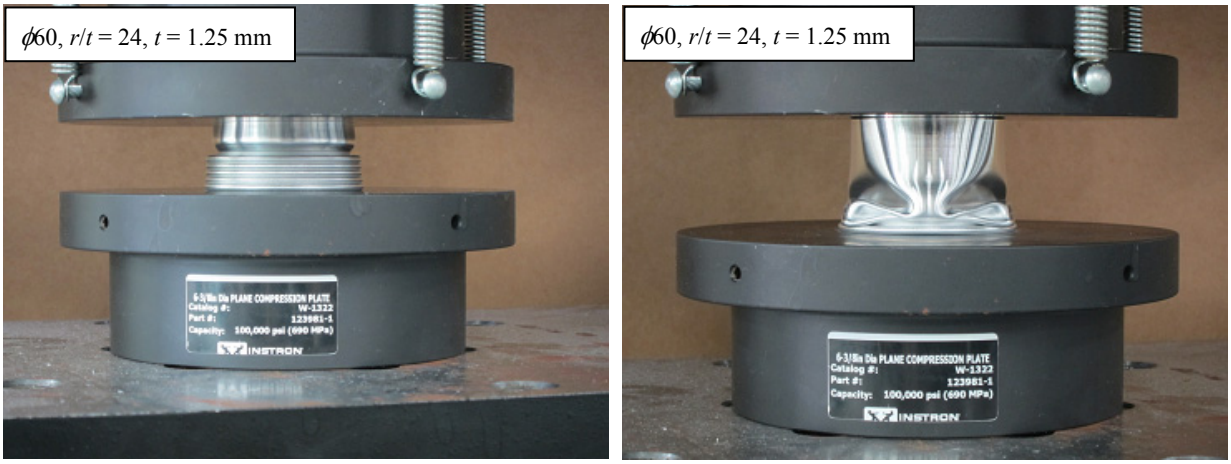

(a) (b)

Fig. 5 Transition from bellows mode to mixed modes with bellows and folding patterns due to *r*/*t*: (a) complete bellows pattern; (b) mixed mode with bellows and folding patterns.

Table 3 Threshold of transition from bellows mode to mixed modes with bellows and folding patterns due to *r*/*t*.

Diameter ϕ	40	50	60
Ratio of *r*/*t*	24	26	24

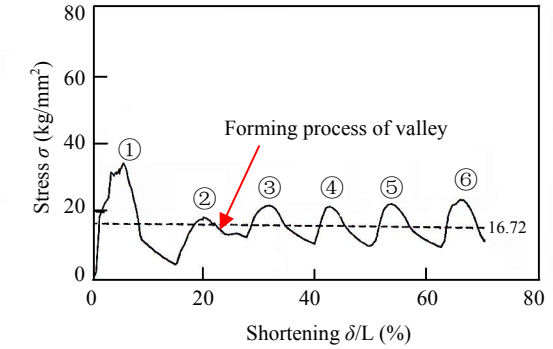

Fig. 6 The relation between stress and strength.

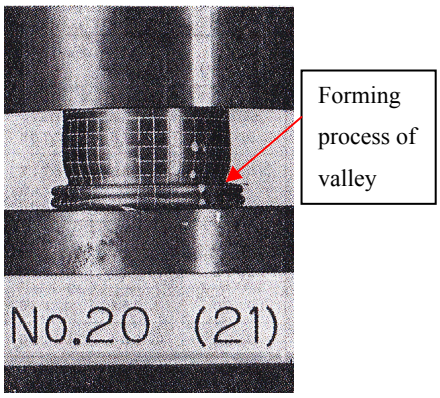

Fig. 7 Experimental crushing process.

5. Conclusions

The test was conducted as quasi-static test with variable *r*/*t* ratio with the Instron-shape equipment, having three types of outer diameter cylindrical pipes with outer diameter kept constant as well as having a condition of without lubrication on both end surfaces. As a result, referring to the *r*/*t* ratio, transition bellow mode to folding mode including bellow mode was clarified. Additionally, regarding uncertain items with previous researches are examined with the following conclusions:

(1) When axial comparison force is loaded, deformation occurs according to a certain spring coefficient *k* within elastic area;

(2) After buckling, the spring coefficient is changed into k' which means, during the process of the first mountain being created, there is a transition range from elastic area to plastic field existing. This is a phenomenon being found in general tension test, however, at the condition of $k \geq k'$;

(3) After buckling, the loading once gets decreased and again increased which goes into a process of valley creation. However, there have been no existing reports about valley creation. Due to Refs. [7, 8], there is a report about quasi-static cylindrical pipes buckling test. Parts of the result are shown in Figs. 6 and 7. A picture of deformation point, which is corresponding to displacement/loading curves, is also shown. In Fig. 3, we can clearly confirm that two mountains are created and the condition of valley creation before the third mountain is being created.

However, there is no description by displacement versus loading curves in the figure. It may be considered due to the performance of test equipment. Valley creation can be confirmed by the inner diameter change. Also, a fact of valley creation means that there is existing energy which is absorption energy;

(4) Buckling behavior is considered an element such as yield stress by changing from elastic to plastic. However, it is confirmed that the behavior is organized by r/t ratio of testing materials. In this case, the value number is around 24;

(5) There are various requirements for designing vehicle body structure. Among them, when vehicle body structures are determined from crash safety stand point, it is important to implement the technical theories that have been studied in order to determine by considering restraint device such as airbags and deceleration. However, it is also necessary to change ideas when different requirement comes out;

(6) From now on, ideas of vehicle body structure is changing from targeting weight reduction by thinning plate structure with large cross-sectional surface to the potential buckling theoretical concept in order to improve efficiency of energy absorption by focusing on shortening a shaft length and offering greater flexibility for other area even though thickness of plate becomes increased;

(7) With what is presented above, it sounds as the weight will be increased, but it should be considered comprehensively.

Acknowledgments

Special thanks to Atom Corporation Fukushima, Fukushima School of Technology and Mr. Hajime Shoji at Iwaki Meisei University in Japan.

References

[1] Structural Strength Crash W/G Committee. 1980. *Creation of Member Disruption Data, Sheet.* Japan: Society of Automotive Engineer of Japan..

[2] Timoshenko, S. P. 1980. *History of Strength of Materials.* Translated by Mogami, T., and Kawaguchi, M. Tokyo: Kashima Publication.

[3] Timoshenko, S. P. 1953. *Theory of Elastic Stability.* Translated by Naka, T. Tokyo: Corona Publication.

[4] Hayashi, T. 1966. *Theory of Light Structure and Its Expansion.* Japan: Japanese Scientists and Engineers.

[5] Matsumoto, K., and Sakurai, T. 2009. *Cylindrical Pipe Bucking Characteristics Aiming for Vehicle Body Frame Collision Characteristic Improvement Research.* Kanto Branch, Society of Automotive Engineers, scholarly lecture presentation.

[6] Sakurai, T., and Matsumoto, K. 2008. "An Experimental Basic Study on Buckling of Cylinders in Order to Improve Crashworthiness of Automotive Vehicles." In *Proceedings of 9th International Conference Technology of Plasticity,* 7-12.

[7] Toi, Y., and Ine, T. 1988. "Basic Studies on the Crashworthiness of Structural Elements." *Axisymmetric Crush Tests of Circular Cylinders and Finite Element Analysis, The Society of Naval Architects of Japan, Paper Collection* 164: 423-36.

[8] Toi, Y., Yuge, K., and Obata, K. 1986. "Basic Studies on the Crashworthiness of Structural Elements." *Non-axisymmetric Crush Tests of Circular Cylinders and Finite Element Analysis, The Society of Naval Architects of Japan, Paper Collection* 160: 296-305.